GEOPHYSICAL RESEARCH LETTERS, VOL. 34, L24S26, doi:10.1029/2007GL031931, 2007

Upscaling river biomass using dimensional analysis and hydrogeomorphic scale-invariance

Elizabeth A. Barnes,[1,2] Mary E. Power,[3] Efi Foufoula-Georgiou,[1] Miki Hondzo,[1] and William E. Dietrich[4]

Received 5 September 2007; revised 24 October 2007; accepted 6 November 2007; published XX Month 2007.

[1] We propose a methodology for upscaling biomass in a river using a combination of dimensional analysis and hydro-geomorphologic scaling laws. We first demonstrate the use of dimensional analysis for determining local scaling relationships between *Nostoc* biomass and hydrologic and geomorphic variables. We then combine these relationships with hydraulic geometry and streamflow scaling in order to upscale biomass from point to reach-averaged quantities. The methodology is demonstrated through an illustrative example using an 18 year dataset of seasonal monitoring of biomass of a stream cyanobacterium (*Nostoc parmeloides*) in a northern California river. **Citation:** Barnes, E. A., M. E. Power, E. Foufoula-Georgiou, M. Hondzo, and W. E. Dietrich (2007), Upscaling river biomass using dimensional analysis and hydrogeomorphic scale-invariance, *Geophys. Res. Lett.*, *34*, L24S26, doi:10.1029/2007GL031931.

1. Introduction

[2] Several studies have related stream periphyton biomass to local physico-chemical characteristics [e.g., *Lowe et al.*, 1986; *Mulholland et al.*, 2001; *Biggs and Gerbeaux*, 1993; *Biggs and Hickey*, 1994; *Biggs*, 1995] as well as to local hydrologic regimes and trophic interactions [e.g., *Power et al.*, 1996; *Wootton et al.*, 1996; *Power and Stewart*, 1987; *Clausen*, 1997]. Algae and cyanobacteria that make up the autotrophic component of periphyton are heterogeneously distributed down river networks, so it remains difficult to quantify their reach or basin-wide abundance, distribution and metabolism. Good estimates of the abundance of algae and cyanobacteria (the primary producers that often dominate periphyton) in rivers and streams are critical for management and restoration of watersheds and water supplies, as well as basic understanding of major energy sources for river food webs.

[3] *Nostoc*, a genus of nitrogen-fixing cyanobacteria, is an important component of periphyton in temperate streams and rivers throughout the world [*Prosperi*, 1989; *Dodds et al.*, 1995]. Where abundant, it is likely a major source of biologically available nitrogen in ecosystems [*Dodds et al.*, 1995]. We demonstrate that a high percentage of the local variability in the height of epiphlithic *Nostoc parmeloides* (45% to 71%) can be explained by hydrologic and geomorphic variables, appropriately grouped via dimensional analysis. We also propose a methodology for combining these local relationships with stream geometry and streamflow scaling to estimate reach-average biomass and its uncertainty. Since these hydro-geomorphic variables can be readily extracted (or computed via hydraulics) from high resolution topography, e.g., LiDaR airborne laser altimetry, the proposed framework offers an attractive way of estimating and upscaling biomass even in regions for which limited biological sampling is available.

2. Study System and Database

[4] An 18 year data set includes measurements of *Nostoc* height and physical stream variables at three cross-stream transects located approximately one kilometer apart along the South Fork Eel River within the Angelo Coast Range Reserve in northern California (Figure 1). The South Fork Eel River experiences a Mediterranean hydrologic regime, with winter floods and summer drought. Further description of this site is given by *Power* [1990, 1992]. Colonies of *Nostoc parmeloides* Kutzing grow attached to bedrock, boulder, and cobble substrates on the river bed. Our index of biomass is 'height' measuring the diameter of a colony if it was spherical, or the major diameter of an ear-shaped, midge-infested colony.

[5] Cross-stream transects were benchmarked at both ends with nails in trees or bedrock (nail to nail distance varied less than 1 cm over repeated surveys). At 0.5 m or 1.0 m intervals across the transect, water depth was measured, and surface velocity was estimated. The modal height of *Nostoc* colonies within an estimated 10×10 cm^2 area around each sampling point on the substrate was recorded (*Power* [1992] and *Power and Stewart* [1987] give further methodological details). *Nostoc* height and stream cross-sectional variables were measured 3 to 20 times each year from 1988–2005 during the growing season (April–August). Table 1 shows the different variables used in this study along with their definitions. It is noted that *Nostoc* biomass can be predicted from the height of the colony through empirical relationships (e.g., M. E. Power, unpublished manuscript, 2006) but these relationships are not directly used in the present study.

[6] Solar radiation (RAD) was measured at the ORLAND2.A weather station (operated by the University of California) approximately 80 miles from the transects. River discharge was measured at the USGS Branscomb gage (USGS 11475500), a decommissioned USGS gage that was reactivated in 1990 by Angelo Reserve researchers,

[1]St. Anthony Falls Laboratory, National Center for Earth-Surface Dynamics, University of Minnesota, Minneapolis, Minnesota, USA.
[2]Now at Department of Atmospheric Sciences, University of Washington, Seattle, Washington, USA.
[3]Department of Integrative Biology, University of California, Berkeley, California, USA.
[4]Department of Earth and Planetary Science, University of California, Berkeley, California, USA.

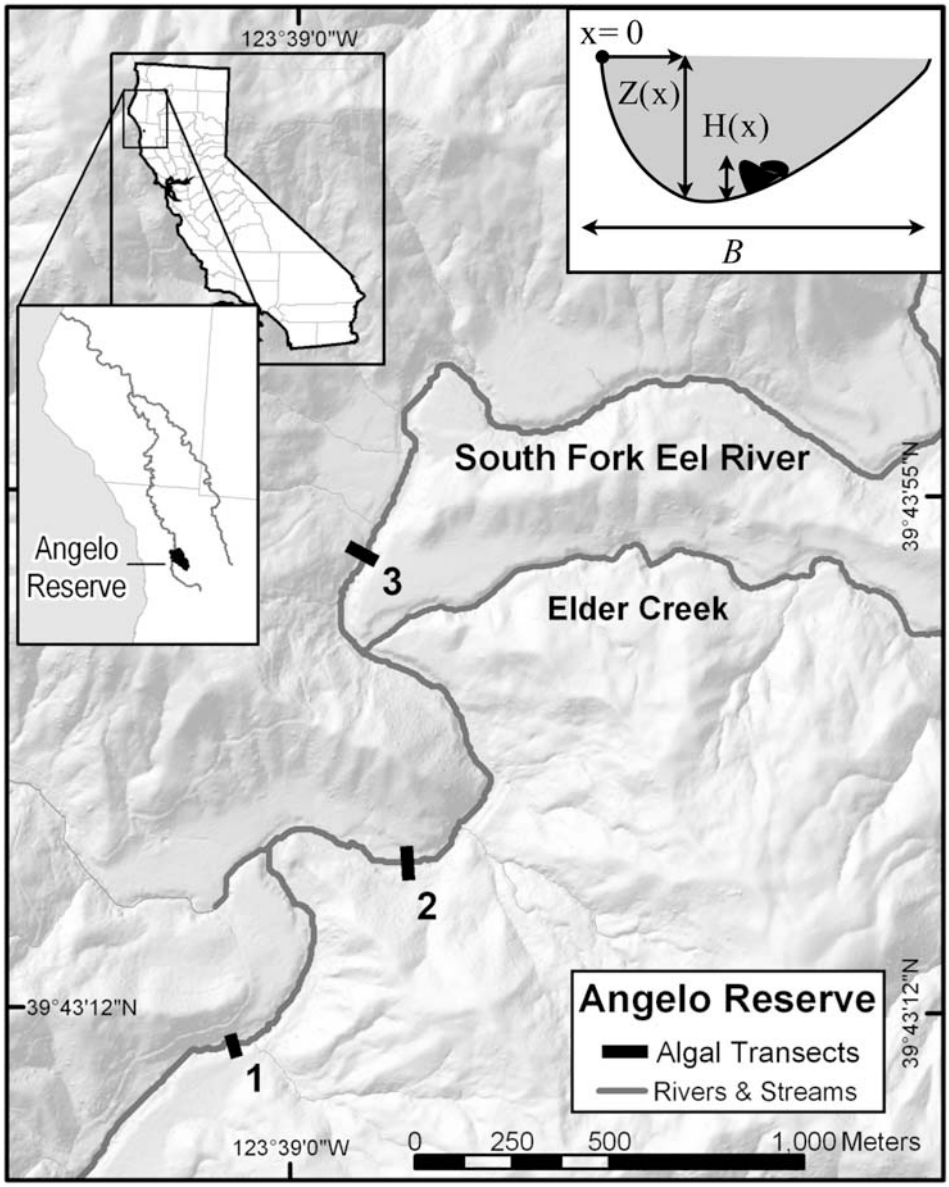

Figure 1. Three transects (1, 2, 3) in the South Fork Eel River, Mendocino County, CA. Transect 1 is the southern most (farthest upstream), while transect 3 is the northern most (farthest downstream) transect. The inset shows a cross-section with relevant variables.

and is located just south of transect 1. Gaps in the hydrologic record from this station were filled with a scaling relationship between discharge at USGS Elder Creek gaging station (USGS 11475560) 4 km away from the Branscomb gage on a major tributary of the South Fork Eel.

3. Terminology and Framework of Analysis

[7] All variables considered in this study are referenced by a location along the river network (s), a location (x) across the considered transect (stream cross-section) and time (t) (see Figure 1). If we denote such a generic variable by $\xi(s, x, t)$, s can be an indexed variable representing the transects 1, 2, and 3; x varies between zero (at the left most position of the cross-section of the transect) and $B(t)$, where $B(t)$ represents the cross-section wetted channel width at time t.

[8] Given the limited data available to quantify environmental controls, a representative quantity for the whole transect is defined as the arithmetic average over all data across the transect. We denote the cross-sectional-averaged quantity with an overbar,

$$\overline{\xi}(s,t) = \frac{1}{B(t)} \int_0^{B(t)} \xi(s,x,t)dx. \quad (1)$$

We relate cross-sectional averaged *Nostoc* colony height, $\overline{H}(s, t)$, to groups of key geomorphic, hydrologic, and other environmental variables which can be observed or estimated. In general, at any transect

$$\overline{H}(s,t) = f_1\left[V_g(s^{\pm}, t^{-}), V_h(s^{\pm}, t^{-}), V_e(s^{\pm}, t^{-})\right] \quad (2)$$

t1.1 **Table 1.** Definitions of Variables

t1.2 Variable	Dimensions	Units	Range[a]	Description
t1.3 $\overline{H}(t)$	L	m	0.001–0.10 (0.005) [0.005]	transect-average *Nostoc* height at time t
t1.4 $\overline{Z}(t)$	L	m	0.06–0.70 (0.28) [0.26]	transect-average water depth at time t
t1.5 $\overline{U}(t)$	LT^{-1}	m/s	0.05–1.61 (0.45) [0.42]	transect-average velocity at time t
t1.6 $B(t)$	L	m	3.00–27.0 (13.5) [8.31]	width of transect at time t
t1.7 RAD	MT^{-3}	kg/s^3	186–715 (260) [303]	average solar radiation (past 45 days)
t1.8 $\rho(t)$	ML^{-3}	kg/m^3	992–998 (996.33) [995.51]	water density ($\propto$ temp) at time t
t1.9 $\overline{U}_{\max}$	LT^{-1}	m/s	0.04–6.88 (1.32) [0.48]	transect-maximum velocity (past 45 days)

t1.10 [a]Spring median in parentheses, summer median in brackets.

where f_1 is a function, V_g denotes a vector of geomorphic variables, V_h a vector of hydrologic variables, and V_e a vector of other environmental variables such as light, temperature and nutrient concentration. In the above relationship, $s^{\pm}$ denotes a location in the vicinity of location s (it would be mostly upstream although a dependence on an immediately downstream junction might be possible), and t^{-} denotes time t and previous times, e.g. dependence on maximum flow in the previous week or dependence on light not only during the specific day of measurement, but during a previous period of time. A dependence on a vector of biotic variables, $V_b(s^{\pm}, t^{-})$, such as grazing could also be added in the above equation but it is not considered in this study.

[9] We assume the geomorphic vector V_g to be composed of B (channel width) and $\overline{Z}$ (channel-averaged depth) (Figure 1); the hydrologic vector V_f to be composed of Q (cross-section average flow) and $Q_{\max}$ (maximum flow over a pre-specified antecedent period), and the environmental vector V_e to be composed of RAD (daily global radiation in W/m^2) and water density as a function of temperature (ρ). From this point on, the time dependence of each variable is implicitly assumed in each equation.

4. Dimensional Analysis

[10] The theory of dimensional analysis is elaborated in many textbooks [e.g., *Potter et al.*, 2002]. The purpose of the analysis is to formulate useful dimensionless groups of variables to describe a process and to establish a basis for similarity between the processes on different time and space scales [*Warnaars et al.*, 2007]. In this paper we use this technique to determine dimensionless groups that provide a basis for explaining *Nostoc* height at different years and transects. The variables chosen for our relationship and their dimensions are given in Table 1. Our generic scaling function takes the following form:

$$\overline{H} = f_2\left(\overline{Z}^a, B^b, \overline{U}^c, RAD^d, \overline{U}_{\max}^e, \rho^h\right). \tag{3}$$

Although a multivariate regression that includes all variables in (3) is possible, the use of dimensional analysis has the advantage of reducing the number of independent variables and resulting in dimension-free parameters.

[11] Inserting the corresponding dimensions (Table 1) into (3), and combining equal dimensions, we obtain:

$$L = L^{a+b+c-3h+e} M^{d+h} T^{-c-3d-e} \tag{4}$$

where L is the dimension of length, M is the dimension of mass and T is the dimension of time. Solving for the above exponents, we derive the dimensionless model to be

$$\left(\frac{\overline{H}}{\overline{Z}}\right) = k\left(\frac{B}{\overline{Z}}\right)^{\alpha}\left(\frac{\overline{U}}{\overline{U}_{\max}}\right)^{\beta}\left(\frac{RAD}{\rho\overline{U}^3}\right)^{\gamma}. \tag{5}$$

The first dimensionless group to the right of the equal sign represents an important geomorphic characteristic of the stream cross-section: width (B) to depth ($\overline{Z}$) ratio. As the width to depth ratio of the channel increases, light becomes more available to *Nostoc*, which, as a nitrogen-fixing autotroph, has a high demand for photosynthetically derived carbon energy. The next dimensionless group captures the cyanobacterium's dependence on moderate (numerator) and high (denominator) stream velocities. Under moderate flow velocities, *Nostoc*, like other attached stream autotrophs, benefits from increasing velocities (increasing flows increase delivery of nutrients and removal of waste products) up to a certain threshold, beyond which scouring, detachment and export occur [*Whitford and Schumacher*, 1964; *Hondzo and Wang*, 2002]. The final dimensionless group is the ratio between solar power (RAD) and stream power per unit stream bed area ($\rho\overline{U}^3$). The exponents α, β, γ and constant k must be determined by fitting (5) with our data.

5. Scaling of *Nostoc* Height

[12] During spring, *Nostoc* colonies re-establish following winter flood scour, and colonies grow, then senesce, during summer. We separated the analysis into two groups: biomass establishment in the spring (April–May) and growth accrual in the summer (June–August). We estimated the parameters of (5) using a weighted linear regression on the logs, with the best fit defined as the minimum sum of squares of the errors and weights inversely proportional to the number of measurements that season. Different time lags were investigated for the definition of $\overline{U}_{\max}$ (see Table 1 for definition), and the highest R^2 was obtained for a time lag of 45 days.

[13] Comparing our data and the proposed scaling relationship (5), we found that the third dimensionless group ($RAD/\rho\overline{U}^3$) contributed an insignificant amount to explaining the variability of the data and it was eliminated from the model. Figure 2 shows the results for transects 1, 2 and 3 over the two seasons. Table 2 shows the results of six other scaling relationships for various seasons and transect combinations. It appears that transects 1 and 2 behave quite

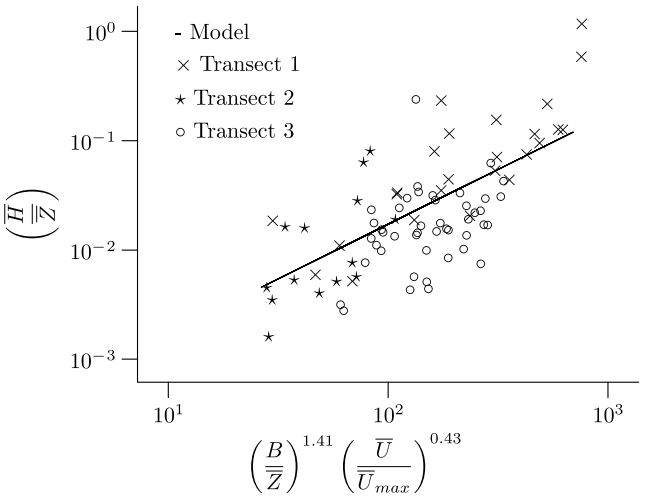

Figure 2. *Nostoc* height over three transects in the spring and summer (April–August) over the 18 years of record. Weighted least squares results in the scaling relationship $\left(\frac{\overline{H}}{\overline{Z}}\right) = 1.7 \times 10^{-4}\left(\frac{B}{\overline{Z}}\right)^{1.41}\left(\frac{\overline{U}}{\overline{U}_{\max}}\right)^{0.43}$ with an $R^2 = 0.45$.

similarly, for 71% of their variability over all seasons was accounted for. *Nostoc* height at transect 3 did not follow the trend depicted by transects 1 and 2, and there are two possible reasons for this. First, transect 3 is located downstream of a major tributary. Second, while transects 1 and 2 have similar valley geometries (symmetric with a slope of approximately 1:8) and thus receive comparable amounts of direct sunlight each day, the flat topography flanking the western shore of transect 3 increased its daily period of insolation. The RAD variable was not able to account for these differences as it was not transect specific and our results show that this radiation variability is not explainable via channel geometry alone (see Table 2 where a lower R^2 was found especially in the summer for transect 3).

6. A Framework for Upscaling Local Biomass

[14] Consider a hypothetical stream reach of 10 km length for which *Nostoc* height observations are available only at a few locations. How is one to estimate the *Nostoc* biomass along the entire stream from the available observations?

[15] Suppose that the *Nostoc* cross-sectional average colony height is scaled by the previously discussed local relationship (5):

$$\overline{H}(s) = k \cdot B(s)^{\alpha} \cdot \overline{Z}(s)^{1-\alpha} \cdot \left(\frac{\overline{U}(s)}{\overline{U}_{\max}(s)}\right)^{\beta} \tag{6}$$

The reach-averaged biomass over a stream reach of length Δs, $\langle \overline{H}(\Delta s) \rangle$, is defined as

$$\langle \overline{H}(\Delta s) \rangle = \frac{1}{\Delta s} \int_{s_0}^{s_0+\Delta s} \overline{H}(s) ds. \tag{7}$$

Due to the nonlinearity of (6), $\langle \overline{H}(\Delta s) \rangle$ cannot be estimated from (6) and (7) by substituting in the reach-averaged quantities $\langle B(s) \rangle$, $\langle \overline{Z}(s) \rangle$, etc. Instead, one must perform integration of (7) by properly acknowledging how each of the variables varies along the stream.

[16] *Leopold and Maddock* [1953] demonstrated that $B(s)$, $\overline{Z}(s)$ and $\overline{U}(s)$ relate to streamflow $Q(s)$ at location s via the so-called hydraulic geometry (HG) relationships:

$$B(s) \propto Q(s)^{m_1} \tag{8}$$

$$\overline{Z}(s) \propto Q(s)^{m_2} \tag{9}$$

$$\overline{U}(s) \propto Q(s)^{m_3} \tag{10}$$

where $m_1 + m_2 + m_3 = 1$. These relationships apply to a specific location for varying flows (at a station HG) or at several locations along a stream for a flow of specific frequency (downstream HG). Since our interest is in integration along a stretch of the stream at a specific instant of time, the downstream HG is relevant for all quantities except for the maximum velocity $\overline{U}_{\max}(s)$ which is considered to result from an extreme flood (e.g., of a specified exceedance probability) at each location and thus at a station HG, $\overline{U}_{\max}(s) \propto Q_{\max}(s)^{m'}3$ needs to be employed. The exponents m_1, m_2, m_3 and m'_3 can be estimated locally (if high resolution topography data are available) or determined using regional relationships [e.g., see *Singh*, 2003]. Substituting these scaling relationships into (6), one obtains,

$$\overline{H}(s) = k' \cdot Q(s)^{M_1} Q_{\max}(s)^{-M_2} \tag{11}$$

where $M_1 = m_1\alpha + m_2(1 - \alpha) + m_3\beta$ and $M_2 = m'_3\beta$. By further introducing the known discharge-drainage area scaling relationships [e.g., see *Gupta and Dawdy*, 1995]

$$Q(s) \propto A(s)^{\theta_1} \tag{12}$$

$$Q_{\max}(s) \propto A(s)^{\theta_2} \tag{13}$$

where θ_1 and θ_2 are exponents dependent on flood frequency and watershed characteristics, we obtain

$$\overline{H}(s) = k'' \cdot A(s)^{p} \tag{14}$$

where $p = \theta_1 M_1 - \theta_2 M_2$. Equation (14) is an approximation of *Nostoc* height at a single transect as a function of

Table 2. Scaling Relationships With R^2 Values for Combinations of Transects and Seasons[a]

Transects and Seasons	α	β	k	R^2
T-1,2,3 spring & summer	1.41	0.43	1.7×10^{-4}	0.45
T-1,2 spring & summer	1.54	0.54	1.8×10^{-4}	0.71
T-3 spring & summer	0.90	0.47	6.9×10^{-4}	0.21
T-1,2 spring	1.70	0.69	0.6×10^{-4}	0.83
T-3 spring	0.14	0.40	172.8×10^{-4}	0.57
T-1,2 summer	1.79	0.62	0.8×10^{-4}	0.71
T-3 summer	0.61	0.52	18.0×10^{-4}	0.22

[a]Functions are of the form $\left(\frac{\overline{H}}{\overline{Z}}\right) = k\left(\frac{B}{\overline{Z}}\right)^{\alpha}\left(\frac{\overline{U}}{\overline{U}_{\max}}\right)^{\beta}$. The amount of variability accounted for by scaling is determined by the R^2 value, as defined by *Draper and Smith* [1981].

upstream drainage area $A(s)$ only, which is easy to extract from maps or digital elevation models. As such, it represents a derived "biological" scaling relationship akin to the hydrologic scaling relationships discussed above, which have found extensive use in hydrology (prediction in ungauged basins and regionalization).

[17] Equation 14 can be further explored for upscaling purposes by noting that $A(s)$ can be related to length $L(s)$ (from the watershed divide to location s) using a variant of Hack's law [e.g., *Rigon et al.*, 1996] for nested basins, $A(s) \propto L(s)^{\delta}$. Combining this with (14) and inserting it into (7), we obtain

$$\left\langle \overline{H}(\Delta s) \right\rangle = k^{*} \cdot \frac{[L^{m+1}(s_0 + \Delta s) - L^{m+1}(s_0)]}{(m+1)\Delta s}. \qquad (15)$$

where $m = \delta(\theta_1 M_1 - \theta_2 M_2)$.

[18] The above relationship quantifies the dependence of reach-averaged biomass on reach length Δs, where the reach starts at an arbitrary location s_0. Assuming without loss of generality that $s_0 = 0$ (i.e. $L(s_0) = 0$ and $L(\Delta s) = \Delta s$), and considering two reaches of lengths Δs_1 and Δs_2, the above relationship results in

$$\frac{\left\langle \overline{H}(\Delta s_1) \right\rangle}{\left\langle \overline{H}(\Delta s_2) \right\rangle} = \left(\frac{\Delta s_1}{\Delta s_2} \right)^{m} \qquad (16)$$

As an illustrative example, let $m_1 = 0.5$, $m_2 = 0.4$, $m_3 = 0.1$ and $m'_3 = 0.3$ (as defined by *Leopold and Maddock* [1953]; see also *Singh* [2003]), $\theta_1 = 1$ and $\theta_2 = 0.7$ [see *Gupta and Dawdy*, 1995, Table V], $\delta = 0.58$ (as extracted by us for the Eel River basin using LiDaR data), $\alpha = 1.41$ and $\beta = 0.43$ (spring and summer *Nostoc* in Table 1); then the final scaling exponent is $m = 0.3$. Thus, if $\Delta s_1 = 10$ km and $\Delta s_2 = 1$ km the above equation implies that *Nostoc* biomass per unit stream length scales by a factor of $10^{0.3} = 2.0$. In other words, starting from a given reference point and going downstream, a stream reach 10 times longer has total *Nostoc* biomass not 10 times, but 20 times larger. Of course, biomass cannot grow unbounded and a physically-imposed upper limit will constrain the range of applicability of the above scaling relationship. Determining this upper limit (empirically or mechanistically) is an issue that requires careful study.

[19] There is uncertainty associated with each HG and flow scaling exponent, and this uncertainty is separate from the errors associated with the model's biomass predictions. To better understand the effects of HG related uncertainties, we performed first order analysis of variance [see *Benjamin and Cornell*, 1970] on (15) with respect to the HG exponents m_1, m_2, m_3, m'_3. Using the values given above, and letting $\Delta s = 1$ km, we find that a 5% uncertainty (standard deviation) in each scaling exponent leads to a 17% uncertainty in the reach-averaged biomass. Of course, as in any uncertainty analysis, it is expected that considering the uncertainly of all variables involved in the model will reduce the power of the predictive relationship.

7. Conclusions and Caveats

[20] We have demonstrated that cyanobacterial biomass scales with hydrologic and geomorphic local variables in a river network (5). Moreover, combining this scaling relationship with hydraulic geometry and other geomorphic and hydrologic scaling laws resulted in a simple nonlinear scaling relationship of transect-averaged biomass with upstream drainage area (14) and stream-averaged biomass with stream length (16). The proposed methodology, which can be further refined in its assumptions, e.g., to consider spatial inhomogeneity in the scaling of HG [see *Dodov and Foufoula-Georgiou*, 2004], can potentially be implemented across different drainage basins and abundances of biota. Being able to upscale local relationships aids in the understanding of the impacts of organisms on ecosystems (e.g. nitrogen loading to river ecosystems by *Nostoc*) as well as how populations are affected by landscape dynamics and heterogeneity. It also aids in efforts to improve (target) field sampling to develop mechanistically-based predictive models of biota at the reach or basin-wide scale by empirically determining the key controlling variables.

[21] In our upscaling example, the HG scaling exponents were assigned "mean regional" values for illustration purposes only. Values specific to each reach should be used to obtain more accurate estimates and thus increase the overall power of the predictive relationships, where the uncertainty can be quantified within the proposed framework.

[22] The distribution and abundance of any species reflect not only whether the environment provides essential resources and tolerable conditions (Fundamental Niche), but also potentially limiting ecological interactions (Realized Niche) [*Hutchinson*, 1957]. *Nostoc* may be more predictable from physical features of its environment than more edible periphyton, because toxic secondary compounds and a tough, mucilaginous sheath deter grazing on this cyanobacterium [*Dodds et al.*, 1995]. Future field work in our system will estimate *Nostoc* biomass over larger areas of the river bed, and relate reach-level biomass to hydraulic scaling parameters and to per-area rates of biological activity (e.g., nitrogen fixation).

[23] **Acknowledgments.** This research was supported by NCED, an NSF SCT funded by the Office of Integrative Activities under agreement EAR-0120914. We thank the University of California Natural Reserve System and the Angelo and Steel families for providing a protected site for this research.

References

Benjamin, J. R., and C. Cornell (1970), *Probability, Statistics and Decision for Civil Engineers*, McGraw-Hill, New York.

Biggs, B. (1995), The contribution of disturbance, catchment geology and land use on the habitat template of periphyton in stream ecosystems, *Freshwater Biol.*, *33*, 419–438.

Biggs, B., and P. Gerbeaux (1993), Periphyton development in relation to macro-scale (geology) and micro-scale (velocity) limiters in two gravel-bed rivers, New Zealand, *N. Z. J. Mar. Freshwater Res.*, *27*, 39–53.

Biggs, B., and C. Hickey (1994), Periphyton responses to a hydraulic gradient in a regulated river in New Zealand, *Freshwater Biol.*, *32*, 49–59.

Clausen, B. B. (1997), Relationships between benthic biota and hydrological indices in New Zealand streams, *Freshwater Biol.*, *38*, 327–342.

Dodds, W., A. Gudder, and D. Mullenbauer (1995), The ecology of Nostoc, *J. Phycol.*, *31*, 2–18.

Dodov, B., and E. Foufoula-Georgiou (2004), Generalized hydraulic geometry: Derivation based on a multiscaling formalism, *Water Resour. Res.*, *40*, W06302, doi:10.1029/2003WR002082.

Draper, N., and H. Smith (1981), *Applied Regression Analysis*, 2nd ed., John Wiley, New York.

Gupta, V., and D. R. Dawdy (1995), Physical interpretations of regional variations in the scaling exponents of flood quantiles, *Hydrol. Processes*, *9*, 347–361.

Hondzo, M., and H. Wang (2002), Effects of turbulence on growth and metabolism of periphyton in a laboratory flume, *Water Resour. Res.*, *38*(12), 1277, doi:10.1029/2002WR001409.
Hutchinson, G. E. (1957), Concluding remarks, *Cold Spring Harbor Symp. Quant. Biol.*, *22*, 415–427.
Leopold, L., and T. J. Maddock (1953), The hydraulic geometry of stream channels and some physiographic implications, *U. S. Geol. Surv. Prof. Pap.*, *252*, 57 pp.
Lowe, R., S. Golladay, and J. Webster (1986), Periphyton response to nutrient manipulation in a clear-cut and forested watershed, *Bull. North Am. Benthol. Soc.*, *3*(2), 77.
Mulholland, P. J., et al. (2001), Inter-biome comparison of factors controlling stream metabolism, *Freshwater Biol.*, *46*, 1503–1517.
Potter, M., D. Wiggert, M. Hondzo, and T. Shih (2002), *Mechanics of Fluids*, 3rd ed., Brooks/Cole, Pacific Grove, Calif.
Power, M. E. (1990), Effects of fish in river food webs, *Science*, *250*, 811–814.
Power, M. (1992), Hydrologic and trophic controls of seasonal algal blooms in northern California rivers, *Arch. Hydrobiol.*, *125*, 385–410.
Power, M., and A. Stewart (1987), Disturbance and recovery of an algal assemblage following flooding in an Oklahoma (USA) stream, *Am. Midland Nat.*, *117*, 333–345.
Power, M., M. Parker, and J. Wootton (1996), Disturbance and food chain length in rivers, in *Food Webs: Integration of Patterns and Dynamics*, edited by G. A. Polis and K. O. Winemiller, pp. 286–297, Chapman and Hall, New York.
Prosperi, C. (1989), The life cycle of Nostoc cordubensis (Nostocaceae, Cyanophyta), *Phycologia*, *28*, 501–503.
Rigon, R., I. Rodriguez-Iturbe, A. Maritan, A. Giacometti, D. Tarboton, and A. Rinaldo (1996), On Hack's law, *Water Resour. Res.*, *32*, 3367–3374.
Singh, V. P. (2003), On the theories of hydraulic geometry, *Int. J. Sediment Res.*, *18*(3), 196–218.
Warnaars, T., M. Hondzo, and M. Power (2007), Abiotic controls on periphyton accrual and metabolism in streams: Scaling by dimensionless numbers, *Water Resour. Res.*, *43*, W08425, doi:10.1029/2006WR005002.
Whitford, L., and G. Schumacher (1964), Effect of a current respiration and mineral uptake in Spirogyra and Oedogonium, *Ecology*, *45*, 168–170.
Wootton, J., M. Parker, and M. Power (1996), Effects of disturbance on river food webs, *Science*, *273*, 1558–1560.

E. A. Barnes, Department of Atmospheric Sciences, University of Washington, 311 ATG Building, Box 351640, Seattle, WA 98195, USA. (eabarnes@atmos.washington.edu)
E. Foufoula-Georgiou and M. Hondzo, St. Anthony Falls Laboratory, National Center for Earth-Surface Dynamics, University of Minnesota, 2 Third Avenue SE, Minneapolis, MN 55414, USA.
W. E. Dietrich, Department of Earth and Planetary Science, University of California, Berkeley, 307 McCone Hall, Berkeley, CA 94720-4767, USA.
M. E. Power, Department of Integrative Biology, University of California, Berkeley, 4184 Valley Life Sciences Building, Berkeley, CA 94720-3140, USA.